Journal of Network Intelligence
Taiwan Ubiquitous Information
 ISSN 2414-8105 (Online)
Volume **8**, Number **4**, November **2023**

2-D GCANet Applied to Denoise 1-D EEG Signals in Online Remote Teaching Scenarios

Ting-Qing Huang

College of Computer and Control Engineering
Minjiang University
No. 200 Xiyuangong Road, Fuzhou University Town, Fuzhou, China
m13115926235@163.com

Chuan-Sheng Wang

Department of Automatic Control Technical
Polytechnic University of Catalonia
Autonomous Region of Catalonia, Barcelona, Spain
wangcs95@163.com

Zhao-Qi Chen

College of Computer and Big Data
Fuzhou University
No. 2 Wulong Jiangbei Avenue, Fuzhou University Town, Fuzhou, China
Zhaoq_chen@163.com

Fu-Quan Zhang*

College of Computer and Control Engineering
Minjiang University
No. 200 Xiyuangong Road, Fuzhou University Town, Fuzhou, China
Digital Media Art, Key Laboratory of Sichuan Province
Sichuan Conservatory of Music
No. 2 Wannianchang Street, Chenghua District, Chengdu City, Sichuan Province, China
Fuzhou Technology Innovation Center of intelligent Manufacturing information System
Minjiang University
NO. 200 Xiyuangong Road, Fuzhou University Town, Fuzhou, China
Engineering Research Center for ICH Digitalization and Multi-source Information Fusion(Fujian Polytechnic Normal University)
Fujian Province University
No. 599 Quanxiu Road, Juyuanzhou Ecological Civilization District, Fuzhou City, Fujian Province, China
zfq@mju.edu.cn

Xiang-Long Meng

College of Electronic Engineering
Shandong University of Science and Technology
No. 579 Qianwangang Road, Huangdao District, Qingdao, China
mengxl99@163.com

Antoni Grau

Department of Automatic Control Technical
Polytechnic University of Catalonia
Autonomous Region of Catalonia, Barcelona, Spain
antoni.grau@upc.edu

Yang Chen

School of Mechanical and Automotive Engineering
Fujian University of Technology
No. 33, Xuefu South Road, University New District, Fuzhou City, Fujian Province

chenyang000515@163.com

Jing-Wei Huang

College of Computer and Big Data
Fuzhou University
No. 2 Wulong Jiangbei Avenue, Fuzhou University Town, Fuzhou, China
m13799974807@163.com

*Corresponding author: Fu-Quan Zhang

Received May 9, 2023, revised July 30, 2023, accepted September 5, 2023.

Abstract. *When EEG signals are used to assess the level of student engagement in online teaching tasks, they are often interfered by noise. It is a challenge to effectively remove these noises. Currently, deep learning methods have been applied to the field of EEG denoising. However, existing methods still have some problems. The denoised signals still have obvious noise residue, or the original EEG signals are damaged, and the model fitting speed is too slow. Image dehazing, as a typical denoising task in the field of image enhancement, has achieved great success in recent years. Therefore, inspired by advanced models in this field, we introduce CNN into EEG denoising tasks. In this paper, we take GCANet, an excellent image enhancement model, as an example. The dilated convolutions and gate fusion subnetworks included in GCANet enable more efficient EEG signal denoising. The results demonstrate that the proposed model effectively reduces noise while preserving essential features. Furthermore, in comparison to other state-of-the-art models, our proposed model exhibits enhanced robustness and faster convergence, as evidenced by achieving lower loss values after five epochs. Its good performance provides a new development idea for the field of EEG denoising.*
Keywords: Deep learning, Neural network, EEG artifact removal, EEG denoising

1. **Introduction.** Online education is a new opportunity created by technological advances for modern education, but it also brings new challenges to teaching efficiency. Teaching across distances makes it difficult for teachers to receive real-time feedback on students' classroom efficiency, which reduces the effectiveness of teaching. Therefore, using EEG signals to extract feedback on students' attention levels has become an effective means for teachers to improve teaching efficiency [1]. However, EEG signals extracted by EEG devices are easily affected by noise interference, which can affect the model's judgment of students' attention levels and make it difficult to provide teachers with effective information. Therefore, it is clearly important to quickly and accurately remove noise and retain the original EEG signals generated by neurons. The noise in EEG signals mainly includes muscle artifact (EMG) [2] and eye artifact (EOG) [3], so this study aims to remove EMG and EOG from EEG signals that are mixed with noise. Figure 1 shows sample segments of EEG signals in the time domain. Figure 2 shows sample segments of f EMG and EOG signals in the time domain. The EOG signal exhibits higher amplitude and lower frequency, while the EMG signal demonstrates higher amplitude and a wider frequency range.

Traditional machine learning methods have been applied in EEG denoising research for a long time [4, 5, 6], but the denoising effect of traditional methods is not ideal, and the output signal has significant distortion. In recent years, with the improvement of computing power, many researchers have introduced deep learning models. The performance of deep learning methods in EEG denoising tasks can be comparable to that of traditional machine learning methods. Currently, a benchmark dataset (EEGdenoiseNet) for end-to-end deep learning solutions for EEG denoising has been proposed by scholars [7], and the

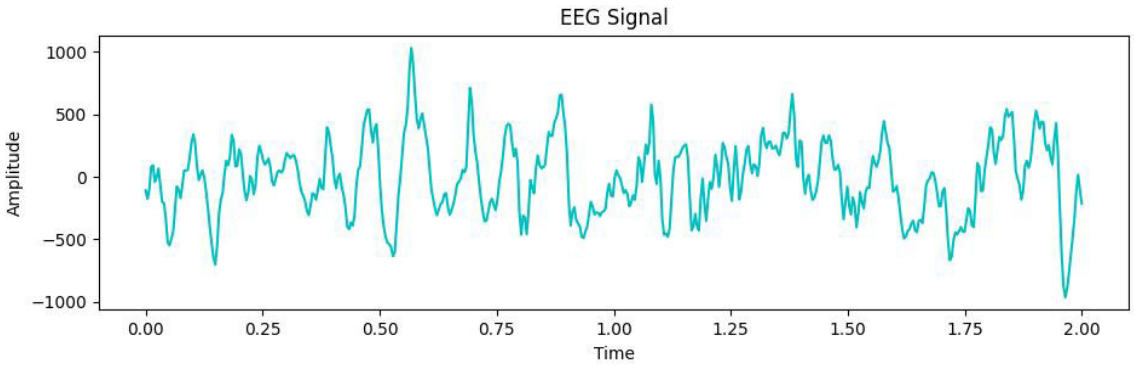

FIGURE 1. Sample Segments of EEG Signals in the Time Domain

denoising performance of four common neural networks (fully connected network, simple and complex convolutional neural networks, and recurrent neural network) has been evaluated on this dataset. However, the current neural network algorithms in the EEG denoising field still have drawbacks such as incomplete removal of noise, destruction of EEG signals leading to distortion, slow fitting speed, which is not conducive to real-time denoising in the future.

In this paper, we take the GCANet algorithm [8] in the field of image enhancement as an example. We convert some 2-D functions in the algorithm to their corresponding 1-D functions and make some parameter adjustments, modifying their original two-dimensional operations to operate along the time dimension, and then use them to denoise EEG signals to investigate whether complex and mature image enhancement algorithms can achieve good results in EEG denoising. We choose GCANet as our research example because: 1) The network is based on CNN, which has been proven to perform well in EEG denoising tasks in previous studies [7]; 2) The model is based on the encoder-decoder framework, which is commonly used in image enhancement algorithms, and is therefore representative. 3) The denoising of EEG signals requires methods that are real-time [9], which requires our method to have high efficiency. Therefore, the model we used is an end-to-end model to achieve real-time denoising.

The model uses convolution kernels of different sizes and dilated convolutions [10], which can simultaneously capture features of different scales and obtain a larger receptive field. We added fully connected layers [11] in the network to obtain more global information. The network also extracts feature information from different levels through the gate fusion subnet to fully utilize information. Therefore, our network has the advantages of fast fitting speed and good denoising effect.

The main contributions of this paper are as follows:

1) We introduced algorithms from 2D image enhancement tasks into 1D EEG denoising tasks, approaching the problem from a new angle , meanwhile providing a fast and effective solution to the challenging task of EEG denoising. Additionally, this approach provides a new idea of borrowing algorithms from similar tasks in different dimensions for future research. This idea can be extended to a wide range of studies.
2) Our method incorporates dilated convolution and feature fusion subnet, which are the innovations of our approach. Dilated convolution helps to increase the receptive field without adding extra parameters and computations.The feature fusion subnet is beneficial for fusing features from different layers, reducing overfitting and accelerating model convergence.
3) The proposed method has been validated to outperform the previous comparative algorithms through qualitative and quantitative analysis. This contributes to the

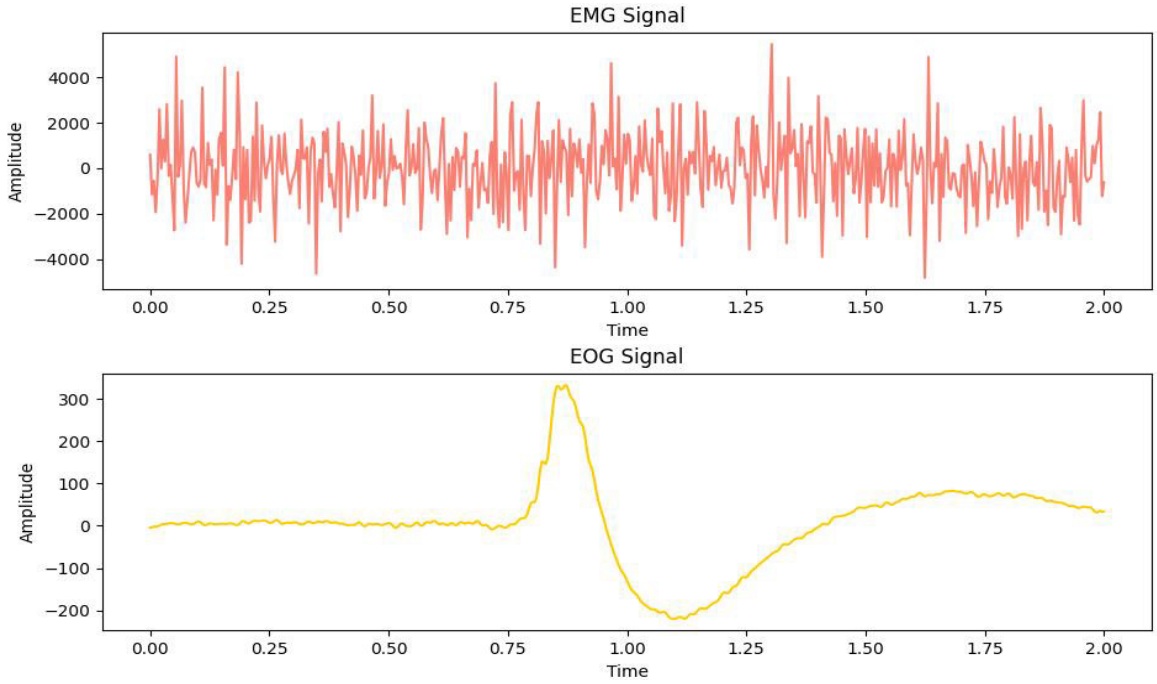

FIGURE 2. Sample Segments of EMG and EOG Signals in the Time Domain

digitalization, intelligence, and efficiency of the education industry, promoting the development of online education.

The structure of the rest of this paper is as follows: First, related work is summarized in Section 2. Second, the specific methods are described in Section 3. Third, the experimental results and analysis are discussed in Section 4, and conclusions are presented in Section 5.

2. **Related Works.**

2.1. **Traditional machine learning methods.** Traditional machine learning denoising algorithms have been applied to EEG denoising, including regression-based methods [4, 12, 13, 14, 15, 16, 17], adaptive filtering-based methods [5, 6, 18, 19], and blind source separation (BSS)-based methods [17, 20, 21, 22, 23, 24, 25, 26]. Firstly, regression-based methods subtract noise templates from noisy EEG, but this method requires good acquisition of noise source signals, which is often difficult. Secondly, adaptive filtering-based methods, such as wavelet transform methods, can transform the original signal from the time domain to the frequency domain. Compared with Fourier transform, it has good time-frequency characteristics and is suitable for analyzing weak and non-stationary signals. BSS-based methods decompose the EEG signals and allocate them to neural sources and artificial sources, and then reconstruct clean signals by recombining the neural components. However, this method can only be used when a large number of electrodes are available, which is not suitable for the single-channel denoising we are studying.However, traditional machine learning methods are difficult to achieve the desired denoising level when applied to EEG denoising.

2.2. **Deep learning methods.** With the development of computing power and the increase in data volume, deep learning has been widely applied in various fields of information technology and has achieved significant results in recent years. For example, Wong et al. proposed a deep learning-based cardiovascular image diagnostic model that overcomes

the challenges of image diagnosis for cardiovascular diseases [27]. Ke et al. developed a deep learning-based human-machine multi-turn language dialogue interaction model, which achieves efficient language interaction [28]. Sanguineti et al. proposed an unsupervised learning-based synthesized acoustic image generation model for audio-visual scene understanding [29]. Wang et al. propose an adaptive fully dense (AFD) neural network for CT image segmentation, achieving excellent results in segmenting CT images with complex boundaries [30]. Wang et al. proposed three deep semantic sorting models based on deep learning, effectively addressing the issues in voice-interaction-enabled industrial central control systems and optimizing the retrieval-based question answering system [31]. Ma et al. proposed a new deep transfer learning architecture, combining convolutional neural networks (CNN) and sparse coding, for false positive reduction in lymph node detection [32]. Zhang et al. proposed a short-term traffic flow prediction algorithm that combines the global optimization capability of quantum genetic algorithm with the simple structure and effective clustering effect of learning vector quantization (LVQ) neural network. This algorithm achieves accurate prediction of traffic flow in urban networks [33].

Deep learning can learn the basic features of neural oscillations hidden in the data and eliminate artifacts from other biological parts [34]. In [7], existing EEG denoising neural networks, including FNN, CNN, CNN with residual blocks, and RNN, were summarized. These neural networks can directly learn the features of noise removal from raw EEG signals.

The following are several classic deep learning algorithms that have been applied to EEG denoising. We will compare them with our proposed algorithm as benchmark algorithms:

Simple CNN: This is a relatively simple convolutional neural network consisting of 4 convolutional blocks. Each block consists of a convolutional layer, a batch normalization layer (BN), and a ReLU layer.The structure is relatively simple, making it easy to implement and train. It has fast computation speed. However, it lacks the ability to model complex noise and signal features.

Complex CNN: Compared to a simple CNN, this algorithm incorporates residual blocks, making the structure more complex. By using residual blocks, it can effectively avoid gradient explosion. In order to extract multi-scale features, we stack residual blocks repeatedly and use 1×3, 1×5, and 1×7 multi-scale convolution kernels. Our algorithm has learned to incorporate this feature.It has higher nonlinear modeling and expressive capabilities. It can better adapt to complex noise and signal structures. However, compared to a simple CNN, the structure is more complex and may require more computational resources and training time.

FCNN: The fully connected network has four hidden layers with ReLU as the activation function. The number of neurons in each layer is equal to the number of time samples in the input signal (512 to reduce eye movement artifacts and 1024 to reduce muscle artifacts). It also includes Dropout regularization to reduce overfitting.It can learn the global dependencies of signals well. However, it may suffer from the curse of dimensionality, especially when the number of time samples in the input signal is large. It struggles to handle long-term dependencies.

Novel CNN: This algorithm contains 7 convolutional blocks with ReLU as the activation function. The first 6 convolutional blocks contain average pooling layers, and the 4th, 5th, 6th, and 7th layers contain Dropout regularization. Finally, there is a flatten operation and a fully connected layer.It has multi-scale modeling capabilities and can adapt to signal structures of different scales. Dropout regularization helps improve the model's generalization ability. However, compared to a simple CNN, the structure is more complex and may require more computational resources and training time.

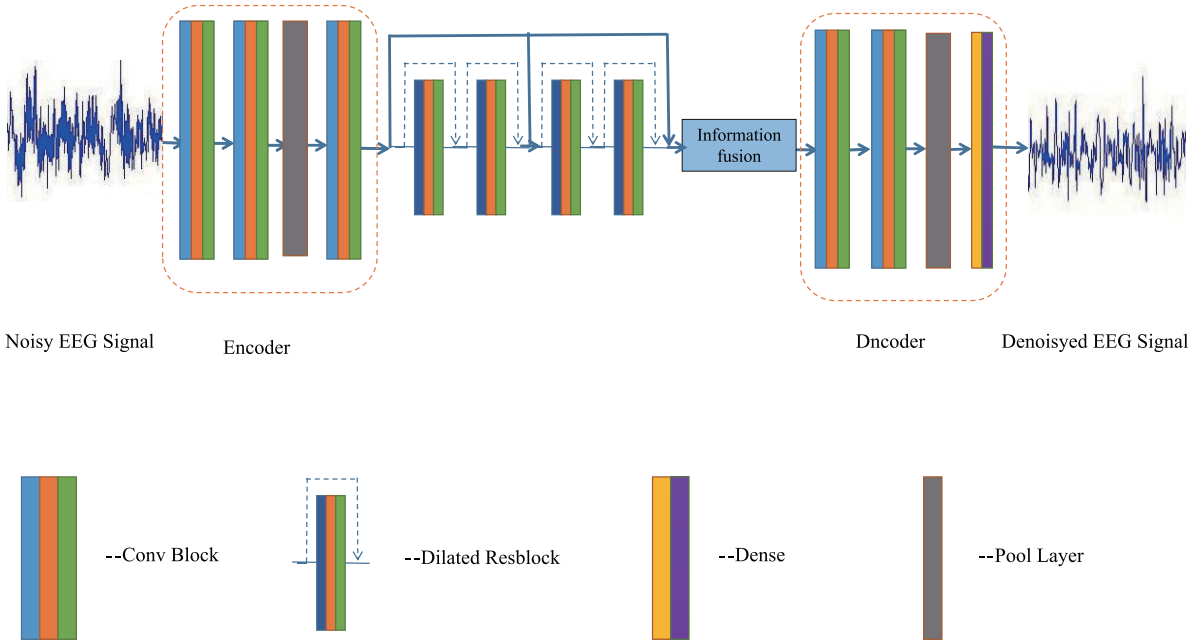

FIGURE 3. Network architecture

RNN (LSTM): The recursive neural network (RNNs) sequentially includes a long short-term memory network (LSTM) that is suitable for analyzing time series features, as well as three fully connected layers with ReLU activation functions and Dropout regularization.It can model time series data and adapt to the evolution of signals at different time steps. It has some memory capacity. However, it may suffer from the problem of vanishing or exploding gradients. Compared to convolutional operations, RNNs may be more time-consuming when processing long sequences.

2.3. **Gate Context Aggregation Network (GCANet).** The Gate Context Aggregation Network (GCANet) is an end-to-end dehazing network that does not rely on prior knowledge. GCANet is an encoder-decoder framework network, composed of convolutional blocks as the encoder part, and deconvolutional and convolutional blocks as the decoder part. Multiple smooth dilated residual blocks are inserted between them to aggregate contextual information and fuse information from different levels. GCANet can predict the target clean image end-to-end and has made significant contributions in the field of image enhancement, solving the problem of grid artifacts.

3. Method.

3.1. **Overall Framework.** In this section, we present the network architecture and denoising methods employed in our study. As illustrated in Figure 3, our model consists of four components: an encoder, Dilated Residual Blocks, Information Fusion, and a decoder. Given a noisy EEG signal, we initially encode it using the encoder. Subsequently, we aggregate more contextual information through four Dilated Residual Blocks. The output of the encoder serves as the input for the first Dilated Residual Block and Information Fusion. The output of the second Dilated Residual Block is simultaneously fed into the third Dilated Residual Block and Information Fusion. The output of the fourth Dilated Residual Block serves as the input for Information Fusion, enabling the fusion of features from different levels. Finally, the output of Information Fusion is decoded to restore the size of the input signal

3.1.1. *Dilated Residual Block.* This paper focuses on dense prediction tasks, which require multi-scale context reasoning and the preservation of spatial resolution information lost during downsampling. Therefore, we use dilated convolutions to achieve a larger receptive field while maintaining resolution [35]. Each Dilated Residual Block contains a dilated convolution and a normalization layer. BatchNormalization [36] is used for the first three Dilated Residual Blocks, as it can speed up the fitting process and prevent overfitting. Layer normalization [37] is used for the fourth Dilated Residual Block, as it is widely used in natural language processing. Considering that EEG signals are one-dimensional, we also use layer normalization here. This approach has been proven feasible in other studies [38].

3.1.2. *Gate Fusion Subnet.* In order to extract features to the maximum extent, we need to fully utilize features from different levels. F_l, F_m, F_h are the outputs of the encoder, the second Dilated Residual Block, and the fourth Dilated Residual Block, respectively. These features can be fused and fed into the decoder through a weighted sum. This process can be represented as:

$$(M_l, M_m, M_h) = G(F_l, F_m, F_h) \tag{1}$$

$$F_o = M_l * F_l + M_m * F_m + M_h * F_h \tag{2}$$

$G(\ ,\ ,\ )$ represents the gating function, and M_l, M_m, M_h are dynamic masks whose values depend on the input features F_l, F_m and F_h at each instance. F_o represents the output feature.

3.1.3. *Network Structure.* Figure 3 shows the network architecture. Given a noisy input EEG signal, the signal is first encoded into feature maps by the encoder. Then, 4 residual blocks, called Dilated Residual Blocks, are inserted between the encoder and decoder. The residual structure can effectively prevent gradient vanishing and exploding, and the dilated convolution aggregates more contextual information. The dilation rates of these 4 residual blocks are set to (2, 4, 4, 1) respectively, and different level features are fused to enhance the learning ability. The enhanced feature information is finally decoded back to the original scale signal as the denoised EEG signal predicted by the network. The orange dashed box in Figure 3 represents the encoder and decoder. Specifically, the encoder uses three convolutional blocks and a pooling layer to encode the input noisy signal into feature maps. Each convolutional block consists of a convolutional layer, a normalization layer, and a ReLU layer. The ReLU layer establishes the non-linear relationship between the layers of the neural network. The convolutional kernels are (1, 3, 5) to extract features of different scales. The decoder consists of two convolutional layers, a pooling layer, and a fully connected layer. The fully connected layer is not used in GCANet, but it can capture global features, while convolutional layers can only capture local features. To make the network perform better, we add a fully connected layer to the end of the network.

3.2. **Denoising Method.** Our proposed method is an end-to-end model, with input being a noisy EEG signal and output being the predicted denoised signal. Our model can be described as a nonlinear mapping function:

$$\hat{x} = F(y, \theta) \tag{3}$$

$$L(x, \hat{x}) = \frac{1}{N} \sum_{i=1}^{N} \|\hat{x}_i - x_i\|_2^2 \tag{4}$$

The variable x represents the clean EEG signal as the ground truth, y represents the noisy EEG signal, $\hat{x}$ represents the predicted denoised signal, and θ represents the learnable

parameters of the neural network. $\hat{x}_i$ represents the i-th sample of the neural network output, and x_i represents the i-th sample of the ground truth x. We also use mean squared error (MSE) as the loss function, which is commonly used in denoising tasks. The error between the predicted denoised EEG signal $\hat{x}$ and the ground truth x, is denoted as $L(x, \hat{x})$. We need to minimize $L(x, \hat{x})$. Refer to Algorithm 1 for details.

Algorithm 1 EEG Denoising

Input: $X_{tra} = \left\{x^i_{tra}\right\}_{i=1,\ldots,n}$ .represents the clean signals as the ground truth for the training set.$Ytra = \left\{y^i_{tra}\right\}_{i=1,\ldots,n}$ .represents the noisy signals for the training set.$Xval = \left\{x^i_{val}\right\}_{i=1,\ldots,n}$represents the clean signals as the ground truth for the validation set.$Yval = \left\{y^i_{val}\right\}_{i=1,\ldots,n}$represents the noisy signals for the validation set.
Output: $F(,\theta)$Trained model with learned weights
Randomly initialize weights θ
repeat
    Use the training set to predict the clean EEG signal $\hat{x}_{tra}$ through $F(y_{tra}, \theta)$
    Calculate the error between the predicted value and the true value using $L(x_{tra}, \hat{x}_{tra})$
    Update θ using the Adam optimizer.
    Using the validation set, predict the clean EEG signal $\hat{x}_{val}$ through $F(y_{val}, \theta)$
    Calculate the error between the predicted value and the ground truth value using $L(x_{val}, \hat{x}_{val})$
until $L(x_{val}, \hat{x}_{val})$converges
return $F(,\theta)$with learned weightsθ, which has undergone training and weight optimization

4. Experiments and Results.

4.1. Experimental Specifications.

All experiments are conducted using TensorFlow 2.2.0 on an Ubuntu 20.04 system, with NVIDIA RTX 3080Ti GPU to optimize the training speed. For each task, we compared with the five contrast algorithm methods separately. All the contrast algorithm models were trained for 60 epochs, and our network model was trained for 5 epochs.By default, we train our model with batch size 40 using the Adam optimizer [39], and the parameter were set to $\alpha = 5\text{e-}5$, $\beta 1 = 0.5$, $\beta 2 = 0.9$. The default initial learning rate is set to 0.00005.

4.2. Dataset.

We used the EEGdenoiseNet dataset [7], which is a dataset suitable for deep neural network-based EEG artifact attenuation. The dataset contains 4514 clean EEG segments as ground truth, 3400 pure EOG segments, and 5598 pure EMG segments as eye and muscle artifact, respectively. It also contains noisy EEG signals synthesized by combining clean EEG segments with artifacts. The process of degrading clean EEG signals into noisy EEG signals can be represented as follows:

$$y = x + \lambda n \tag{5}$$

$$SNR = 10 \log_{10} \frac{RMS(x)}{RMS(x \cdot n)} \tag{6}$$

$$RMS(g) = \sqrt{\frac{1}{N} \sum_{i=1}^{N} g_i^2} \tag{7}$$

y represents a one-dimensional mixed signal of EEG and artifact; x represents the clean EEG signal as the ground truth; n represents (ocular or muscle) artifact; λ is a hyperparameter that controls the signal-to-noise ratio (SNR) of the contaminated EEG signal y. A lower λ corresponds to a higher SNR, meaning less noise added; conversely, a higher

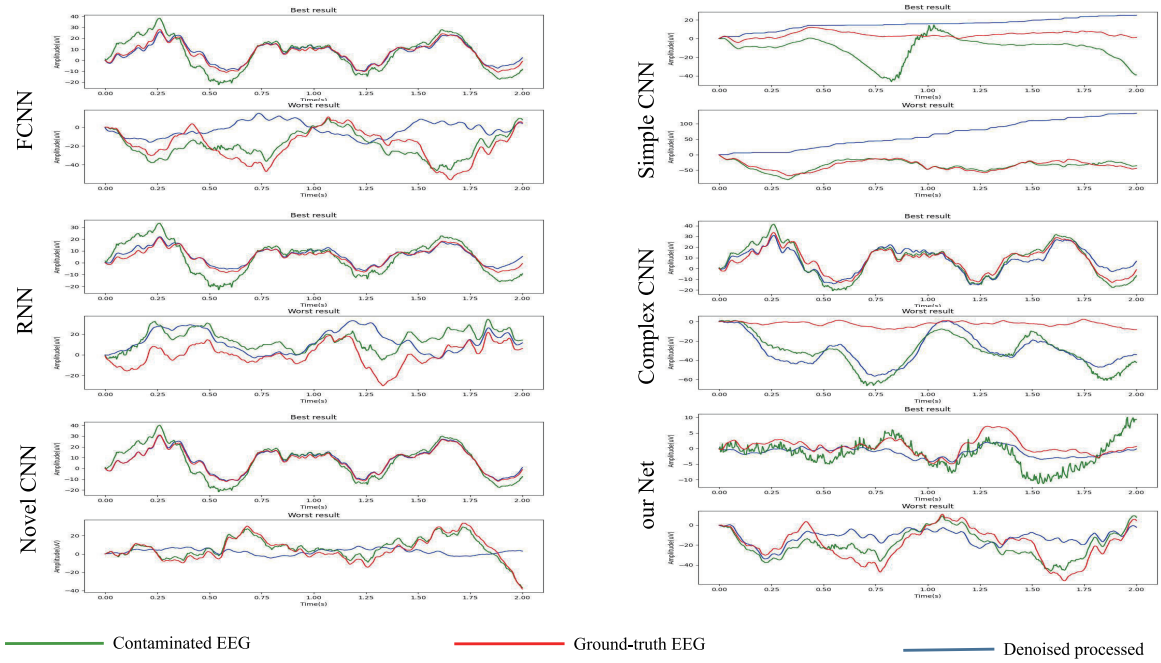

FIGURE 4. Removing Muscle-Related Artifacts in Time Domain

λ corresponds to a lower SNR, meaning more prominent noise. The calculation of the root mean square (RMS) is given by Equation (7), where there are N time samples in a segment g, and the i-th sample in g is denoted by g_i.

4.3. **Comparisons with State-of-the-art Methods.** We compared our proposed method with several deep learning-based EEG denoising method.Similar to [7], we compare the proposed model with the methods including: Simple CNN , Complex CNN , FCNN , Novel CNN , RNN(LSTM) .

4.3.1. *Qualitative Analysis.* We conducted a qualitative analysis of the network performance by displaying some sample segments in the time domain. We showed some sample segments in the time domain to remove muscle-related artifacts (Figure 4) and eye-related artifacts (Figure 5). For each network and noise type, we displayed two segments: the best result and the worst result. It can be seen that during the removal of eye and muscle-related artifacts, the artifacts are significantly attenuated, and the EEG signals are well reconstructed.

4.3.2. *Quantitative Analysis.* To quantitatively analyze the network's performance in different frequency bands, we calculated the power ratio of the signal in different frequency bands. Table 1 and Table 2 illustrate the power ratio of the signal in different frequency bands for six different denoising algorithms, including five comparison algorithms and our algorithm, as well as the ground truth and noisy EEG. Each row of data corresponds to one algorithm, and each column of data corresponds to one frequency band. The six frequency bands are Delta (1-4 Hz), Theta (4-8 Hz), Alpha (8-12 Hz), Beta (12-30 Hz), and Gamma (30-100 Hz).

In Table 1, the noise is EMG, and our algorithm performs best in the Delta and Theta frequency bands and overall achieves better results than other algorithms in other frequency bands.

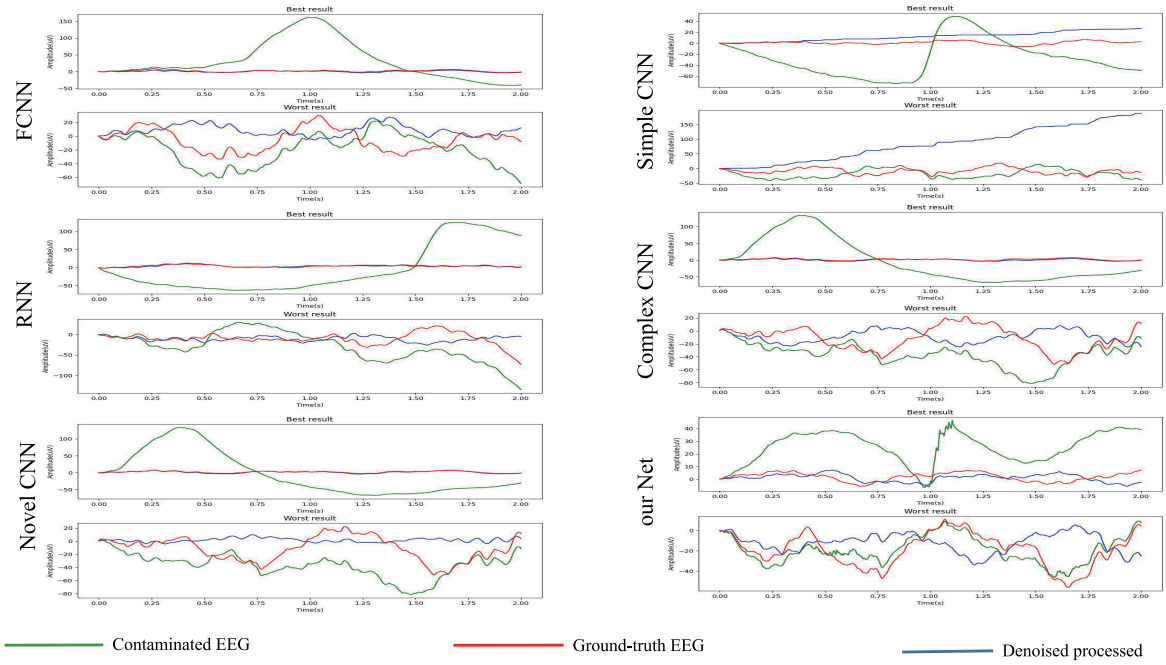

FIGURE 5. Removing Eye-Related Artifacts in Time Domain.

In Table 2, the noise is EOG, and our algorithm performs less well in the Beta and Gamma frequency bands but still performs better than some other algorithms in other frequency bands.

Comparing the performance of our network in different noise environments, our network performs better when the noise is EMG but less well when the noise is EOG. Overall, our algorithm performs well, but its performance may be compromised in handling different types of noise.

To quantitatively analyze the network performance, we measured its convergence by analyzing the loss values on the validation set during training. Table 3 shows a table of loss values for our algorithm and 5 comparison algorithms on the EMG and EOG denoising tasks. The smaller the loss value, the better the network's denoising performance. Our Net was trained for only 5 epochs, and the corresponding loss value in the table is its loss value at the 5th epoch, while the other networks were trained for 60 epochs, and the corresponding loss value in the table is their loss value at the 60th epoch. Our Net achieved lower loss values of 0.133 and 0.127 for the EMG and EOG denoising tasks, respectively, which is lower than other networks and indicates that Our Net has good robustness in denoising tasks. From the perspective of fitting speed, Our Net has a faster fitting speed.

5. **Conclusion.** In order to enable teachers to better determine students' level of concentration during online classes through EEG signals, this article proposes a network for EEG denoising. To effectively remove EMG and EOG noise from EEG, we introduce the GCANet image enhancement algorithm. The dilated convolution module is beneficial for expanding the receptive field, and the feature fusion subnetwork module is beneficial for the model to learn features at different levels.By comparing with five advanced EEG denoising methods on the EEGdenoisnenet dataset.our method proves to be more efficient in removing interference noise from electroencephalograms and retaining more complete original EEG signals. It is evident that incorporating 2D image enhancement algorithms

TABLE 1. Power ratios of different frequency bands before and after myogenic artifact removal

Denoising method	delta	theta	alpha	beta	gamme
FCNN	0.207	0.151	0.070	0.207	0.365
RNN	0.215	0.165	0.076	0.210	0.335
Simple CNN	0.201	0.182	0.081	0.213	0.323
Complex CNN	0.149	0.130	0.067	0.216	0.438
Novel CNN	0.258	0.182	0.069	0.197	0.293
Ours	0.215	0.183	0.079	0.208	0.315
Ground Truth	0.235	0.206	0.090	0.211	0.259
Contaminated signal	0.098	0.097	0.057	0.223	0.524

TABLE 2. Power ratios of different frequency bands before and after ocular artifact removal

Denoising method	delta	theta	alpha	beta	gamme
FCNN	0.246	0.191	0.081	0.205	0.278
RNN	0.237	0.195	0.084	0.206	0.278
Simple CNN	0.210	0.185	0.083	0.218	0.303
Complex CNN	0.232	0.199	0.083	0.212	0.273
Novel CNN	0.270	0.195	0.078	0.201	0.257
Ours	0.169	0.149	0.068	0.213	0.401
Ground Truth	0.235	0.206	0.090	0.211	0.259
Contaminated signal	0.098	0.095	0.057	0.236	0.514

TABLE 3. Final test loss value for each network

method / dataset	FCNN	RNN	Simple CNN	Complex CNN	Novel CNN	Ours
EMG	0.195	0.146	0.412	0.232	0.195	0.127
EOG	0.197	0.116	0.433	0.170	0.190	0.133

into 1D EEG denoising is a research direction with huge potential. Our research has accelerated the development of EEG denoising. Moving forward, we will investigate how to further improve and optimize the existing EEG denoising network.In the future, we will attempt to introduce more algorithms for similar tasks of different dimensions into 1D signal denoising.

Acknowledgment. This work was jointly supported by the project of Digital Media Art, Key Laboratory of Sichuan Province (Sichuan Conservatory of Music, Project No. 21DMAKL01), the first batch of industry-university cooperation collaborative education project funded by the Ministry of Education of the People's Republic of China (Minjiang University, Project No. 202101071001), Minjiang University 2021 school-level scientific research project (Minjiang University, Project No. MYK21011), Open Fund Project of Fuzhou Technology Innovation Center of Intelligent Manufacturing Information System (Minjiang University, Grant No. MJUKF-FTICIMIS2022), Open Fund Project of Engineering Research Center for ICH Digitalization and Multi-source Information Fusion (Fujian Polytechnic Normal University, Grant No. G3-KF2204), Guiding Project of Fujian Province (Minjiang University, Project No. 2020H0046), Key Technology Research and Industrialization Project for Software Industry Innovation in Fujian Province (MinjiangUniversity and Fujian Guotong Information Technology Co., Ltd., Project No. 36),Spanish MINECO national project with reference (PID2019-106702RB-C21 /AEI / 10.13039/501100011033). The authors also gratefully acknowledge the helpful comments and suggestions of the reviewers, which have improved the presentation.

REFERENCES

[1] T. Zhang, Y. Li, and J. Dong, "Eeg-based attention level recognition during online learning," *Journal of Educational Technology Development and Exchange*, vol. 9, no. 1, pp. 1–14, 2016.

[2] S. D. Muthukumaraswamy, "High-frequency brain activity and muscle artifacts in meg/eeg: a review and recommendations," *Frontiers in Human Neuroscience*, vol. 7, p. 138, 2013.

[3] R. J. Croft and R. J. Barry, "Removal of ocular artifact from the eeg: a review," *Neurophysiologie Clinique/Clinical Neurophysiology*, vol. 30, no. 1, pp. 5–19, 2000.

[4] B. W. McMenamin, A. J. Shackman, J. S. Maxwell, D. R. Bachhuber, A. M. Koppenhaver, L. L. Greischar, and R. J. Davidson, "Validation of ica-based myogenic artifact correction for scalp and source-localized eeg," *Neuroimage*, vol. 49, no. 3, pp. 2416–2432, 2010.

[5] P. He, G. Wilson, and C. Russell, "Removal of ocular artifacts from electro-encephalogram by adaptive filtering," *Medical and Biological Bngineering and Computing*, vol. 42, pp. 407–412, 2004.

[6] P. He, G. Wilson, C. Russell, and M. Gerschutz, "Removal of ocular artifacts from the eeg: a comparison between time-domain regression method and adaptive filtering method using simulated data," *Medical and Biological Engineering and Computing*, vol. 45, pp. 495–503, 2007.

[7] H. Zhang, M. Zhao, C. Wei, D. Mantini, Z. Li, and Q. Liu, "Eegdenoisenet: A benchmark dataset for deep learning solutions of eeg denoising," *Journal of Neural Engineering*, vol. 18, no. 5, p. 056057, 2021.

[8] X. Li, T. Wu, J. Deng, L. Jie, S. Liu, W. Wu, and H. Luo, "Gated context aggregation network for image dehazing and deraining," *IEEE Transactions on Image Processing*, vol. 29, pp. 9234–9248, 2020.

[9] K.-K. Tseng, C. Wang, T. Xiao, C.-M. Chen, M. M. Hassan, and V. H. C. de Albuquerque, "Sliding large kernel of deep learning algorithm for mobile electrocardiogram diagnosis," *Computers & Electrical Engineering*, vol. 96, p. 107521, 2021.

[10] F. Yu and V. Koltun, "Multi-scale context aggregation by dilated convolutions," *arXiv preprint arXiv:1511.07122*, 2015. [Online]. Available: https://arxiv.org/abs/1511.07122

[11] D. E. Rumelhart, G. E. Hinton, and R. J. Williams, "Learning representations by back-propagating errors," *Nature*, vol. 323, no. 6088, pp. 533–536, 1986.

[12] P. He, M. Kahle, G. Wilson, and C. Russell, "Removal of ocular artifacts from eeg: a comparison of adaptive filtering method and regression method using simulated data," in *2005 IEEE Engineering in Medicine and Biology 27th Annual Conference*. IEEE, 2006, pp. 1110–1113.

[13] B. W. Mcmenamin, A. J. Shackman, J. S. Maxwell, D. R. W. Bachhuber, A. M. Koppenhaver, L. L. Greischar, and R. J. Davidson, "Validation of ica-based myogenic artifact correction for scalp and source-localized eeg," *Neuroimage*, vol. 49, no. 3, pp. 2416–2432, 2010.

[14] G. Gratton, M. G. Coles, and E. Donchin, "A new method for off-line removal of ocular artifact," *Electroencephalography and Clinical Neurophysiology*, vol. 55, no. 4, pp. 468–484, 1983.

[15] R. J. Croft and R. J. Barry, "Eog correction: Which regression should we use?" *Psychophysiology*, vol. 37, no. 1, pp. 123–125, 2000.

[16] B. W. McMenamin, A. J. Shackman, J. S. Maxwell, L. L. Greischar, and R. J. Davidson, "Validation of regression-based myogenic correction techniques for scalp and source-localized eeg," *Psychophysiology*, vol. 46, no. 3, pp. 578–592, 2009.

[17] M. A. Klados, C. Papadelis, C. Braun, and P. D. Bamidis, "Reg-ica: a hybrid methodology combining blind source separation and regression techniques for the rejection of ocular artifacts," *Biomedical Signal Processing and Control*, vol. 6, no. 3, pp. 291–300, 2011.

[18] M. Hemmatifard and M. Eidiani, "Mehdi hemmatifard-removal of ocular artifacts from electro encephalogram by adaptive filters-persian," Technical Report, January 2015. [Online]. Available: https://doi.org/10.13140/RG.2.1.2413.4481

[19] Z. Weidong and L. Yingyuan, "Eeg multiresolution analysis using wavelet transform," in *2001 Conference Proceedings of the 23rd Annual International Conference of the IEEE Engineering in Medicine and Biology Society*, vol. 2. IEEE, 2001, pp. 1854–1856.

[20] X. Chen, X. Xu, A. Liu, S. Lee, X. Chen, X. Zhang, M. J. McKeown, and Z. J. Wang, "Removal of muscle artifacts from the eeg: A review and recommendations," *IEEE Sensors Journal*, vol. 19, no. 14, pp. 5353–5368, 2019.

[21] S. Wold, K. Esbensen, and P. Geladi, "Principal component analysis," *Chemometrics and Intelligent Laboratory Systems*, vol. 2, no. 1-3, pp. 37–52, 1987.

[22] A. Hyvärinen and E. Oja, "Independent component analysis: algorithms and applications," *Neural Networks*, vol. 13, no. 4-5, pp. 411–430, 2000.

[23] S. Makeig, A. J. Bell, T.-P. Jung, and T. J. Sejnowski, "Independent component analysis of electroencephalographic data," *Advances in Neural Information Processing Systems*, vol. 8, no. 8, pp. 145–151, 1996.

[24] M. Corsi-Cabrera, M. A. Guevara, Y. D. Río-Portilla, C. Arce, and Y. Villanueva-Hernández, "Eeg bands during wakefulness, slow-wave, and paradoxical sleep as a result of principal component analysis in the rat," *Sleep*, vol. 24, no. 6, pp. 738–744, 2000.

[25] K. Sweeney, S. McLoone, and T. Ward, "The use of ensemble empirical mode decomposition with canonical correlation analysis as a novel artifact removal technique," *IEEE Transactions on Biomedical Engineering*, vol. 60, no. 1, pp. 97–105, 2013.

[26] X. Chen, C. He, and H. Peng, "Removal of muscle artifacts from single-channel eeg based on ensemble empirical mode decomposition and multiset canonical correlation analysis," *Journal of Applied Mathematics*, vol. 2014, 2014.

[27] K. K. Wong, G. Fortino, and D. Abbott, "Deep learning-based cardiovascular image diagnosis: a promising challenge," *Future Generation Computer Systems*, vol. 110, pp. 802–811, 2020.

[28] X. Ke, P. Hu, C. Yang, and R. Zhang, "Human–machine multi-turn language dialogue interaction based on deep learning," *Micromachines*, vol. 13, no. 3, p. 355, 2022.

[29] V. Sanguineti, P. Morerio, A. Del Bue, and V. Murino, "Unsupervised synthetic acoustic image generation for audio-visual scene understanding," *IEEE Transactions on Image Processing*, vol. 31, pp. 7102–7115, 2022.

[30] E. K. Wang, C.-M. Chen, M. M. Hassan, and A. Almogren, "A deep learning based medical image segmentation technique in internet-of-medical-things domain," *Future Generation Computer Systems*, vol. 108, pp. 135–144, 2020.

[31] K. Wang, C.-M. Chen, M. S. Obaidat, S. Kumari, S. Kumar, and J. Long, "Deep semantics sorting of voice interaction-enabled industrial control system," *IEEE Internet of Things Journal*, vol. 10(4), pp. 2793–2801, 2021.

[32] Y. Ma, Y. Peng, and T.-Y. Wu, "Transfer learning model for false positive reduction in lymph node detection via sparse coding and deep learning," *Journal of Intelligent & Fuzzy Systems*, vol. 43, no. 2, pp. 2121–2133, 2022.

[33] F. Zhang, T.-Y. Wu, Y. Wang, R. Xiong, G. Ding, P. Mei, and L. Liu, "Application of quantum genetic optimization of lvq neural network in smart city traffic network prediction," *IEEE Access*, vol. 8, pp. 104 555–104 564, 2020.

[34] Y. U. Khan, S. M. Anwar, and M. Majid, "Eeg signal analysis: A survey," *Journal of Medical Systems*, vol. 43, no. 8, p. 233, 2019.
[35] F. Yu and V. Koltun, "Multi-scale context aggregation by dilated convolutions," *arXiv preprint arXiv:1511.07122*, 2016.
[36] S. Ioffe and C. Szegedy, "Batch normalization: Accelerating deep network training by reducing internal covariate shift," *arXiv preprint arXiv:1502.03167*, 2015.
[37] J. L. Ba, J. R. Kiros, and G. E. Hinton, "Layer normalization," *arXiv preprint arXiv:1607.06450*, 2016.
[38] P. Yi, K. Chen, Z. Ma, D. Zhao, X. Pu, and Y. Ren, "Eegdnet: Fusing non-local and local self-similarity for 1-d eeg signal denoising with 2-d transformer," *arXiv e-prints*, 2021.
[39] D. P. Kingma and J. Ba, "Adam: A method for stochastic optimization," *arXiv preprint arXiv:1412.6980*, 2014. [Online]. Available: https://arxiv.org/abs/1412.6980